THE AMERICAN MINERALOGIST, VOL. 55, SEPTEMBER-OCTOBER, 1970

HYDROTHERMAL ALTERATION IN CORE FROM RESEARCH DRILL HOLE Y-1, UPPER GEYSER BASIN, YELLOWSTONE NATIONAL PARK, WYOMING[1]

S. HONDA, *Mining College, Akita University, Akita-shi, Japan*
AND L. J. P. MUFFLER, *U.S. Geological Survey, Menlo Park, California 94025.*

ABSTRACT

Y-1 penetrated an active hot-spring system to 215 feet (65.5 m), where the temperature was 171°C. The core is sinter to 12 feet (3.7 m), sandstone, conglomerate, and siltstone composed of rhyolite detritus to 211 feet (64.3 m), and bedrock rhyolite.

Hydrothermal minerals replace obsidian and fill open spaces. Original plagioclase and alkali feldspar are unaltered. Clinoptilolite, mordenite, opal, and relic α-cristobalite occur in the less altered core. In the more intensely altered core analcime is the sole zeolite, hydrothermal quartz is abundant, and α-cristobalite has been converted to quartz. Montmorillonite and celadonite occur throughout most of the core; calcite, pyrite, muscovite, kaolinite, erionite, and aegirine are sporadic. Hydrothermal alkali feldspar occurs in only one sample.

Associated hot-spring fluids are dilute, slightly alkaline, and contain mainly Na, Cl, HCO_3, and SiO_2.

Major factors controlling formation of hydrothermal minerals in Y-1 are 1) nature of starting material, 2) elevated temperature, and 3) fluid composition. Parallel distribution patterns of zeolites and silica species suggest that variation in SiO_2 activity is important.

Hydrothermal alteration in Y-1 has produced mineral assemblages similar to those produced during low-temperature diagenesis of sedimentary rocks rich in volcanic detritus.

INTRODUCTION

This report describes the core from Y-1, a diamond drill hole in Upper Geyser Basin, Yellowstone National Park. Y-1 is one of 13 research drill holes completed by the U.S. Geological Survey in 1967 and 1968 in Yellowstone Park. The drill collar is at an elevation of 7294 feet on the east side of the Black Sand loop road at Black Sand Basin, 40 feet at S. 77° E. of a periodically discharging spring known as Whistle Geyser (Fig. 1). The hole is now filled with cement and capped.

Y-1 was spudded April 18, 1967 and reached a maximum depth of 215 feet (65.5 m) on April 24, 1967. Water was used as the circulating fluid. Core diameter was 4.5 inches from 0 to 21 feet, 2.36 inches from 21 to 100 feet, and 1.72 inch from 100 to 215 feet. Core recovery was by wireline method and averaged 84 percent.

The core, generally taken in 5 or 10 foot intervals, was logged by Muffler and D. E. White as soon as possible after acquisition. At this time approximately 25 percent of the core was selected for laboratory study.

[1] Publication authorized by the Director, U.S. Geological Survey.

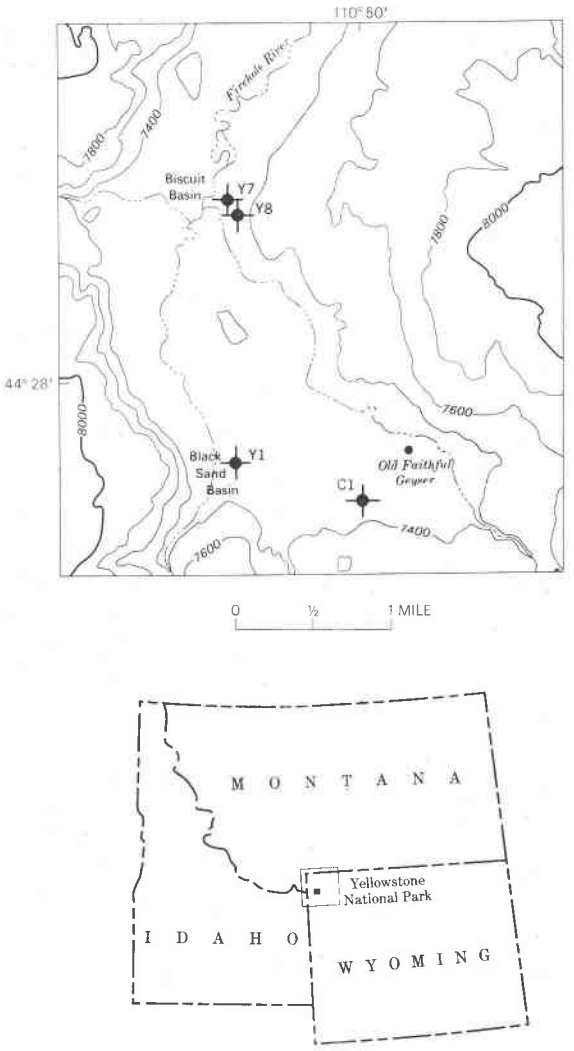

FIG. 1. Map showing locations of drill holes, Upper Geyser Basin. Y-1, Y-7, and Y-8 were drilled by the U.S. Geological Survey in 1967. C-1 was drilled by the Carnegie Institution in 1929 (Fenner, 1936).

Selected samples either contained unusual features (*e.g.*, veins, vugs, contacts, textural relations) or were representative of an interval. Most of the analytical data reported in this paper were determined from this "skeleton" core; the bulk core was put in storage and referred to only for detailed study of contact zones.

Detailed optical and X-ray study of the skeleton core was carried out in the U.S. Geological Survey Menlo Park laboratories. Sixty thin sections and over 400 X-ray diffractograms were studied. We wish to acknowledge the assistance of Mrs. Terry E. C. Keith and Miss Chere Barnett in these laboratory studies.

Temperature data taken at the hole bottom as drilling progressed are given on Figure 2. Profiles acquired in this manner closely approximate predrilling ground temperature, whereas temperatures measured in the open hole after completion may be very misleading (unpublished Yellowstone drilling data of D. E. White, R. O. Fournier, L. J. P. Muffler, and A. H. Truesdell). Temperatures above the reference boiling point curve at depths greater than 125 feet on Figure 2 do not imply an absence of liquid water; correction for water overpressure indicates that both water and steam are present at these depths. Water overpressure measured at the wellhead reached a maximum of approximately 31 psig.

Fluid samples uncontaminated by drill water were not obtained before the drill hole had to be plugged by cement. Nearby springs of Black Sand Basin, however, discharge near-neutral waters containing dominantly Na, Cl, HCO_3, and SiO_2 (Table 1). By analogy with other Yellowstone drill holes from which we were able to collect fiuid samples, we expect that deep samples from Y-1 would have shown the same general chemistry as waters derived from nearby hot springs. The silica content given in Table 1 indicates an underground reservoir temperature of approximately 200°C (Fournier and Rowe, 1966).

Y-1 is 4,630 feet west-northwest of the Upper Basin hole drilled to a depth of 406 feet by the Carnegie Institution in 1929 (Fenner, 1936). The Carnegie hole (C-1 on Fig. 1) penetrated the same glacial deposits and rhyolite flow as Y-1 (see below) and reached a maximum temperature of 180°C. Alteration in C-1 was similar to that in Y-1 except for the abundant adularia reported from C-1 but identified in only one specimen from Y-1. We have not yet restudied the Carnegie core, and shall not attempt a detailed comparison with Y-1.

Stratigraphy

The depositional units penetrated by Y-1 are shown in columnar section at the left of Figure 2. The shallowest 12 feet is sinter—amorphous silica deposited on the ground surface by flowing thermal water. The sinter contains diatom tests, displays plant casts, and shows textural features indicating the presence of algae at the time of deposition. Sinter is currently being deposited throughout Black Sand Basin.

From 12 feet to approximately 207 feet the drill hole penetrated interbedded sandstone, conglomerate, and siltstone that have been cemented by hydrothermal action. These rocks comprise a unit locally termed "black sand," which occurs throughout most of Upper Geyser Basin. Where unaltered and uncemented by hot-spring action, the unit is characterized by nearly spherical sand grains and granules of black obsidian. The spherical

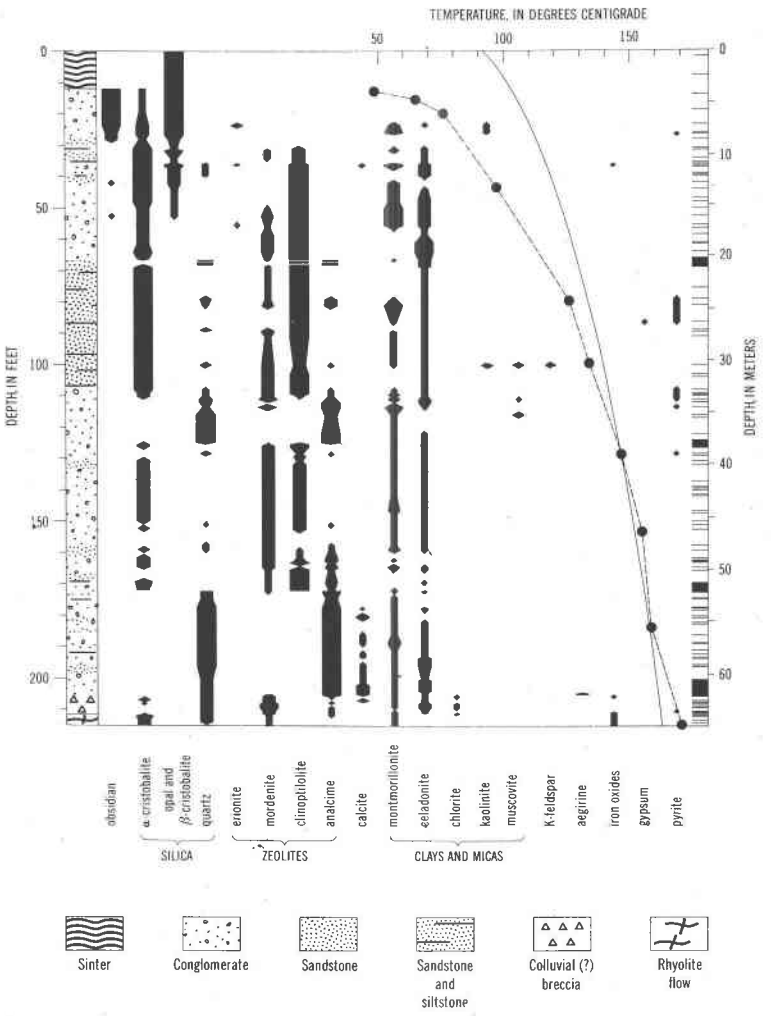

FIG. 2. Distribution of fresh obsidian, devitrification α-cristobalite, and hydrothermal alteration minerals in Y-1. Column on left shows generalized stratigraphic section penetrated by Y-1 (see text). Horizontal lines at right indicate samples selected for skeleton core and studied in detail; the four solid bars indicate intervals studied in too much detail to show individual samples. Width of the mineral columns is an estimate of relative abundance based on X-ray diffraction data. Interpolation between data points assumes linear variation in abundance except when a mineral abundance goes to zero, in which case the zero point is arbitrarily put no more than one foot from the last occurrence. The dashed line connects data points of bottom-hole temperatures. Boiling point curve is for pure water everywhere at boiling, assuming water level at the surface (7,294 feet) and no water overpressure.

TABLE 1. CHEMICAL ANALYSIS OF SPOUTER GEYSER, 425 FEET N. 53° W. OF Y-1

	ppm
SiO_2	313
Al	.5
Fe	1
Ca	1
Mg	1
Na	425
K	20
Li	3.3
HCO_3	454
CO_2	75
SO_4	18
Cl	312
F	35
B	3.6
Total	1662

Sample taken September, 1962. Analyst: J. J. Rowe. Boron value on sample taken September, 1961. Silica value determined in field September, 1961 by R. O. Fournier. Temperature of geyser, 92°C, pH = 8.8.

shapes are due to the result of hydration fractures in the glass. Pebbles and cobbles in the gravel layers are varicolored lithoidal rhyolite having a devitrified groundmass composed of alkali feldspar and silica (α-cristobalite or quartz). Sporadic cavities in the lithoidal rhyolite contain crystals of tridymite and alkali feldspar which were deposited from vapor during cooling of the rhyolite flow from which the clasts were derived. Quartz, sanidine (approximately $Ab_{50}Or_{50}$), minor andesine, and sporadic clinopyroxene occur as phenocrysts in the obsidian and lithoidal rhyolite and as detrital grains derived from phenocrysts.

Bedding throughout the sedimentary rocks in Y-1 is conspicuous except in the thicker conglomerate beds. Dips commonly are less than 10° but locally range up to 30°. Cross beds and graded beds are common, and several pieces of core display contorted zones that may represent slumping before induration. The siltstone and sandstones, particularly in the interval from 70 to 110 feet, display fractures that offset bedding as much as several centimeters. These fractures commonly are healed by hydrothermal cementation, but some larger ones have central void space up to 2 mm measured perpendicular to the fracture. Core from 70 to 90 feet has two apparently conjugate sets of fractures; the steep set has reverse offset, and the shallow set, normal offset.

These sedimentary rocks probably were deposited as outwash sediments during the waning stages of early Pinedale Glaciation (H. Waldrop, pers. commun., 1969). Using the correlation chart given as Table 2 of Richmond (1965), the early Pinedale Glaciation took place approximately 20,000 to 25,000 years B. P. The obsidian detritus that makes up the bulk of these sediments probably was derived from the obsidian-rich flow just west of Upper Geyser Basin. This flow has not been dated, but stratigraphic correlation with other flows that have been dated suggests eruption approximately 100,000 years ago (R. L. Christiansen, pers. commun., 1969)

At a depth of 207 feet in Y-1 the sedimentary section passes gradationally downward

into a coarse colluvial (?) breccia and thence at 211 feet into a rhyolite flow characterized by abundant phenocrysts of corroded andesine. K-Ar dating of this flow by J. D. Obradovich (R. L. Christiansen, 1969, pers. commun.) gives an age of 525,000 years.

Hydrothermal alteration. The rocks encountered in Y-1 have been markedly affected by interaction with hot water. Except at the shallowest levels, the rhyolite obsidian has been converted to zeolites, clay minerals, and silica. These hydrothermal minerals are also abundant in open spaces and as fracture fillings.

Sanidine and plagioclase phenocrysts are sharply bounded and unaltered (Fig. 3), with only one exception (100 feet). In some samples even

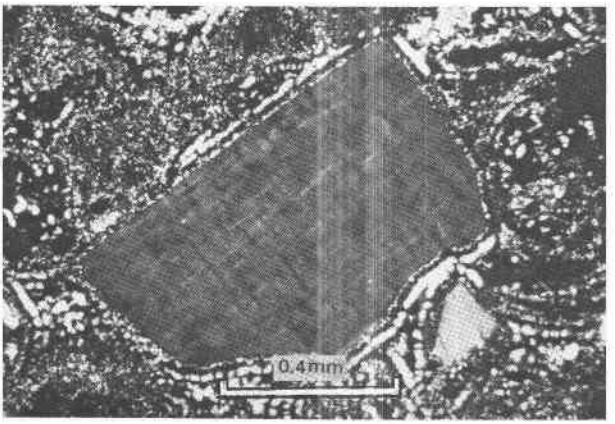

FIG. 3. Photomicrograph of Y1-125, showing unaltered crystal of microperthitic sanidine surrounded by clinoptilolite that replaces obsidian clasts and fills intergranular space. Crossed polars.

remnants of the sporadic clinopyroxene phenocrysts can be detected, but these clearly have been partly converted to clay minerals.

The lithoidal rhyolite fragments also show little hydrothermal alteration. Many clasts display a plumose fine intergrowth of alkali feldspar and α-cristobalite, both of which are products of devitrification during cooling of the flow material from which the clasts were derived. In the more intensely altered zones of Y-1, however, this α-cristobablite has crystallized to quartz, with preservation of the plumose texture. The correlation of these quartz-bearing lithoidal clasts with the analcime-rich intensely altered zones of Y-1 indicates that the quartz is a recrystallization product and not an original devitrification product. The alkali feldspar in these devitrified rocks shows no microscopic indication of hydrothermal alteration, but its chemical composition has not been investigated.

The distribution of obsidian, devitrification α-cristobalite, and hydrothermal minerals in Y-1 is shown on Figure 2 as a function of depth. Phenocryst minerals and devitrification alkali feldspar are present in all samples deeper than 12 feet and are not shown.

The shallowest 12 feet of Y-1 is opaline sinter. Opal also occurs as secondary filling of voids and fractures in the initially very porous sinter. The contact between the sinter and the underlying conglomerate was not recovered in the core, but it was marked by a change in color of return water from white to dark gray at 12 feet.

From 12 feet to approximately 30 feet, the core is a sporadically indurated gravel rich in sand grains and granules of black obsidian. Opal

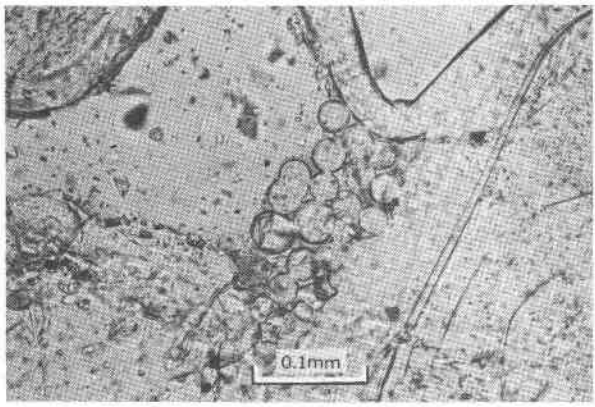

FIG. 4. Photomicrograph of Y1-19, showing spherical habit of opal. Plane light.

occurs primarily as transparent, vitreous crusts lining intergranular cavities and cementing the clasts. The habit is commonly botryoidal, and in some samples opal occurs as minute spheres (Fig. 4). Refractive index of the opal ranges from 1.43 to 1.45, and X-ray diffractograms show a broad maximum from 19° to 25° $2\theta_{Cu}$. Some samples show partial crystallization to β-cristobalite, which is detected by a broad X-ray peak at approximately 21.8° $2\theta_{Cu}$. We interpret this β-cristobalite to have been produced by solid-state crystallization of initial opal deposited by the hot water, but the possibility of direct crystallization from the hydrothermal solutions can not be excluded. Vitreous opal also occurs at 14 feet as a thin coating on a gently dipping irregular fracture. A white clay-like material along this fracture also proved to be opal.

Other hydrothermal minerals occur only in trace amounts in this zone. Celadonite, montmorillonite, and traces of kaolinite occur as thin films between clasts and the opal cement and along hydration cracks in the obsidian. Minute cubes of pyrite are deposited on opal at 26.5 feet. The

only zeolite detected in this zone is erionite, which occurs sporadically with montmorillonite and opal at 23.5 feet. To our knowledge this is the first reported occurrence of erionite in a hot-spring system.

A major alteration boundary occurs at approximately 30 feet, but the contact relations are unknown owing to the recovery of only 0.3 feet of core between 27.5 and 30.5 feet depth. From 30 to 66.5 feet the core consists of conglomerate, sandstone, and minor siltstone that are generally light grayish-green. With the exception of the core at 42 and 52.5 feet,

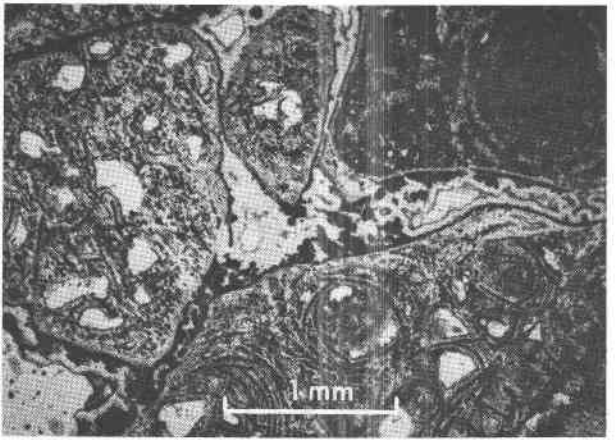

FIG. 5. Photomicrograph of Y1-61.5, showing relict perlite cracks marked by montmorillonite in fragments of obsidian that have been completely replaced by clinoptilolite. Clinoptilolite and botryoidal celadonite also occur in intergranular space. Plane light.

fresh obsidian is absent, having been altered mainly to clinoptilolite. Mordenite occurs in open spaces at 31.5 and 34 feet, and is common at depths greater than 50 feet. Erionite was detected in trace amounts at 36 and 55.5 feet. Both celadonite and montmorillonite are common. Opal and β-cristobalite are abundant in the shallow parts but they were not detected below 52.5 feet. Calcite occurs in intergranular cavities at 36 and 36.5 feet, and quartz occurs in fissures and vugs with β-cristobalite from 36 to 39.5 feet.

Clinoptilolite, the characteristic alteration mineral of this zone, occurs as replacement of obsidian, as lining of intergranular cavities (Fig. 5), and in fractures. Where growing in open spaces, the clinoptilolite occurs as stubby, euhedral crystals 0.02 to 0.10 mm in size that have a megascopic saccharoidal aspect. Clinoptilolite that replaces obsidian has a fibrous habit. Obsidian clasts replaced by clinoptilolite retain the relict perlitic structure as outlined by montmorillonite and/or celadonite (Fig. 5).

The grayish green color of this zone is due primarily to celadonite. In

thin section this meneral is a brilliant green. It occurs along relict hydration cracks, in pumice vesicles and as botryoidal growths extending into the intergranular void space (Fig. 5). Some relict obsidian clasts are brown.

The pattern of alteration to a mineral association dominated by clinoptilolite is interrupted by two bands of analcime-rich rock at 66.5–66.9 feet and 67.35–68.05 feet. Clinoptilolite and mordenite are absent in these zones. The sole zeolite is analcime, which is associated with abundant hydrothermal quartz. α-cristobalite could not be detected in the analcime-bearing layers or in clinoptilolite-bearing rocks within approximately 3 inches of the analcime-bearing layers. Celadonite is persistent throughout the interval, but montmorillonite is absent or present only in trace amounts from 58 to 78 feet.

Boundaries of the analcime-bearing layers are parallel to bedding in the sandstones but irregular and only rudely parallel to bedding in the conglomerates. There are no fractures in the rock and no major primary lithologic breaks that could have localized the boundaries. Contacts in hand specimen are marked by a sharp line between gray-green clinoptilolite-bearing rock and dark-green analcime-bearing rock. In thin section, however, analcime occurs on the clinoptilolite side of the boundary, decreasing in abundance rapidly away from the contact.

The analcime occurs as isotropic crystals 0.1 to 0.2 mm in diameter that sporadically show 6-sided form. Where analcime replaces volcanic fragments, the original perlitic texture of the hydrated obsidian is obliterated. Analcime also occurs in intergranular cavities. Hydrothermal quartz occurs as lozenges or prisms 15×30 microns enclosed by or surrounding analcime.

The interval from 68.05 to 111 feet consists of sandstone and siltstone with only a few conglomerate beds. Clinoptilolite replacing obsidian clasts and lining intergranular cavities is again the dominant alteration mineral. Cottony mordenite is common in open spaces. Celadonite occurs throughout the interval whereas montmorillonite is sporadic. All samples studied contain α-cristobalite.

Complexly banded, steeply dipping fracture fillings up to 5 mm thick occur at 79 feet and from 108 feet to 110 feet. These fracture fillings display symmetrical bounding zones 0.4 to 2.0 mm thick that are composed entirely of clinoptilolite. Banding parallel to the fracture margins (Fig. 6) is caused by variation in grain size from 0.005 mm to 0.5 mm. The larger crystals of clinoptilolite are oriented perpendicular to the banding or form clusters radiating outward towards the center of the fracture (Fig. 7). The central parts of the fracture fillings are texturally complex mixtures

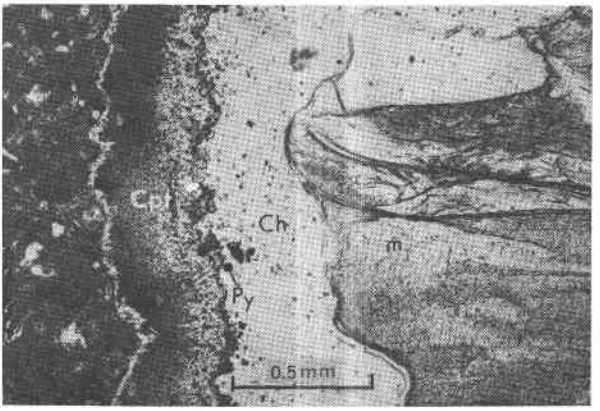

FIG. 6. Photomicrograph of Y1-109, showing edge of fracture filled with clinoptilolite (cpt), chalcedony (ch), pyrite (py), and montmorillonite (m). Matrix at left is a fine-grained sandstone rich in clinoptilolite and mordenite. Banding in clinoptilolite zone is due to variation in grain size. Plane light.

of montmorillonite, chalcedony (Fig. 6), mordenite, pyrite, analcime, and open space. Analcime crystals locally coalesce to monomineralic bands up to 0.8 mm thick (Fig. 7).

Other fractures do not contain analcime. At 81 feet a fracture 8 mm wide is lined with chalcedony upon which was deposited mordenite and montmorillonite; the central part of the fracture is void space. Steeply dipping, irregular fractures coated with montmorillonite occur at 89.5

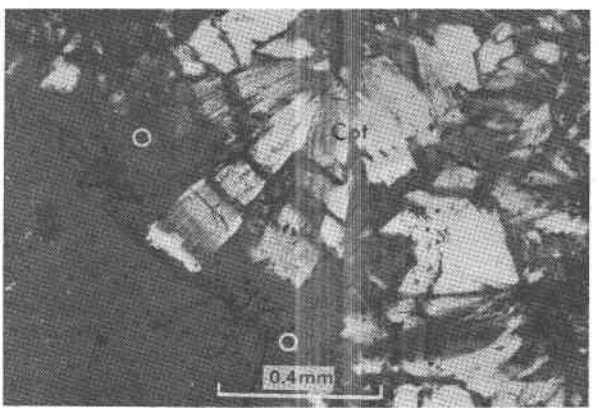

FIG. 7. Photomicrograph of Y1-79, showing radiating sheaves of clinoptilolite (cpt) overgrown by analcime (o) at edge of fracture filling. Partly crossed polars.

and 91 feet, and at 89 feet there is a fracture filling of pure chalcedony 0.5 mm thick. At 86.5 feet a thin fracture dipping 20° is lined with pyrite, montmorillonite, and traces of gypsum. The available experimental data (Holland, 1967, p. 418-419) indicate that anhydrite should be the stable calcium sulfate at temperatures greater than 57°C. Inasmuch as the temperature in Y-1 at 86.5 feet is about 129°C (Fig. 2) this gypsum either was formed metastably or was produced subsequent to drilling by oxidation of pyrite.

The drill core at 100 feet is a sandstone that contains a single rhyolite cobble 5 cm in diameter. This cobble has a light-gray to violet central

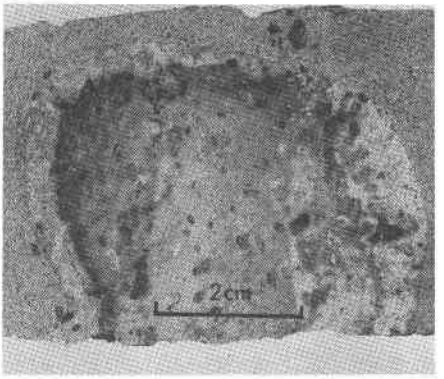

FIG. 8. Photograph of Y1-100, showing rhyolite cobble in fine-grained sandstone rich in clinoptilolite. White alteration rim is dominantly potassium-rich hydrothermal alkali feldspar.

part surrounded by a bleached rim 1 to 10 mm in thickness (Fig. 8). This rim is difficult to explain other than as a reaction rim caused by hydrothermal alteration after the cobble was incorporated in the sandstone.

The sandstone contains the usual clinoptilolite-mordenite-celadonite-montmorillonite mineral association, and the constituent grains of detrital feldspar are, as usual, unaltered. The cobble, however, is unique in Y-1 for its bewildering variety of alteration minerals and their enigmatic textural relations.

Sanidine phenocrysts both in the central part of the cobble and in the rim are veined and partly altered to clinoptilolite. Other feldspar phenocrysts in the central part of the cobble are completely replaced by clinoptilolite, kaolinite, and muscovite(?). Quartz phenocrysts are unaltered. The groundmass of the central part of the cobble is a murky aggregate of tridymite, clinoptilolite, kaolinite, analcime, mordenite, quartz, and alkali

feldspar; the tridymite commonly occurs in nests and is most probably relic from high-temperature vapor-phase crystallization. The rim of the cobble, on the other hand, has an aphanitic groundmass made up of dominant K-feldspar, subordinate clinoptilolite and quartz, and minor mordenite and analcime. Interpretation of X-ray diffraction powder data (Table 2) using Figure 1 of Wright and Stewart (1968) indicates this K-feldspar to be essentially pure potassium end member and of high-sanidine structural state. This high K content contrasts strikingly with the intermediate compositions of the phenocrysts and devitrification alkali feldspars of the Yellowstone rhyolites and suggests formation or recrystallization at hydrothermal temperatures rather than vapor-phase or devitrification temperatures (*cf.* solvus of Orville, 1963, Fig. 9).

TABLE 2. CELL PARAMETERS OF MONOCLINIC K-FELDSPAR FROM RIM OF COBBLE IN Y1-100

$a =$	$8.594 \pm .0029$ Å
$b =$	$13.023 \pm .0055$ Å
$c =$	$7.178 \pm .0028$ Å
$V =$	721.36 Å^3
$\beta =$	$116°7.0'$
Total standard errors =	$.026°2\theta$
Lines used =	17

Values are calculated from X-ray diffractometer data using a computer program modified from Evans, Appleman and Handwerker (1963).

Possible explanations for this cobble are speculative. Perhaps, as suggested by A. J. Gude, 3rd (written comm., 1969), the cobble was altered to zeolites before it was incorporated into the early Pinedale gravels, and the K-feldspar-rich rim resulted from further reaction with the hydrothermal fluids at the Y-1 site.

In contrast to most other alteration boundaries in Y-1, the contact at 111 feet is along a fracture. This fracture dips approximately 80°, and its walls are 6 mm apart. It is filled with analcime, chalcedony, montmorillonite, pyrite, muscovite, celadonite, and mordenite, but no clinoptilolite. Complex banding within the fracture is produced by modal variations in the filling material, and there is void space about 1 mm across at the center. The sandstone of the hanging wall is greenish gray, soft, and contains abundant clinoptilolite and mordenite but only sporadic analcime. The rock of the footwall, on the other hand, is a medium gray, tough sandstone rich in analcime and hydrothermal quartz, with no clinoptilolite or mordenite.

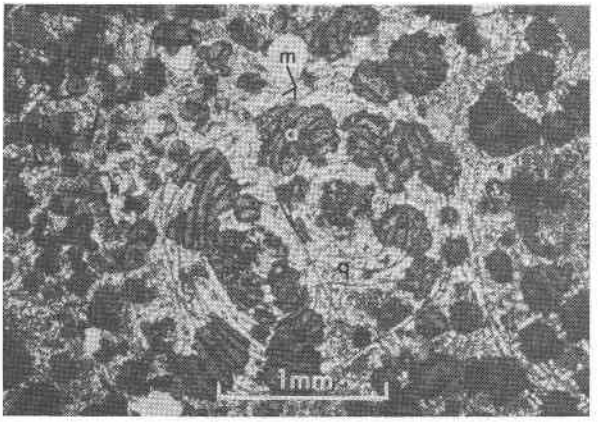

FIG. 9. Photomicrograph of Y1-111, showing relict perlite cracks marked by montmorillonite (m) in obsidian fragments completely altered to analcime (a) and quartz (q). Partly crossed polars.

The dominant alteration assemblage from 111 to 125 feet is analcime-quartz. The quartz occurs both as interlocking crystals averaging 0.03 mm surrounding euhedral analcime crystals (Fig. 9), and as lozenge-shaped crystals 0.01–0.05 mm enclosed in analcime (Fig. 10). Although many of these tiny crystals have a habit similar to that of adularia, extinction is always parallel to the long axis and sporadic hexagonal cross sections give uniaxial positive figures. Beam scans on an electron microprobe by M. H. Beeson showed that these crystals in core from 117 feet contain no Al, K, or Na, thus confirming the identification as quartz. The recrystal-

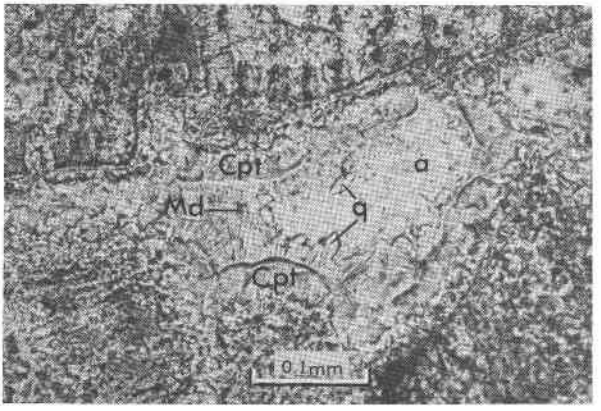

FIG. 10. Photomicrograph of Y1-125.0, showing mordenite (md), quartz (q), and analcime (a) in an intergranular cavity lined with clinoptilolite (cpt). Clasts are obsidian replaced by clinoptilolite. Plane light.

lization to analcime-quartz partly or wholly obliterates the relic perlite structure (Fig. 9).

α-cristobalite is absent in this zone. Fragments of lithoidal rhyolite display the characteristic plumose structure but are composed of alkali feldspar and quartz.

At 116 feet the drill core displays a mass about 4×5 cm that consists of relict obsidian clasts altered to nearly pure muscovite in a matrix of quartz and muscovite. The top of the mass shows rude control by a bedding plane, but the other margins of the mass show no apparent lithologic or structural control. Plagioclase and sanidine phenocrysts throughout both the muscovite-bearing mass and the analcime-bearing remainder of the sample are microscopically unaltered. Comparison of X-ray diffraction data with that given by Yoder and Eugster (1955) suggests that this muscovite has the 1M structure.

The lower contact of the analcime-quartz zone at 125.0 feet is a sharp boundary dipping about 15°. As is the case for the contacts in the 66–69 foot interval, the boundary is not controlled by any fracture or primary lithologic discontinuity. In the rock just above the 125.0 foot contact, analcime occurs both as open-space filling and replacement of obsidian. Analcime persists for 2 inches into the clinoptilolite-bearing rock below, but only as open-space filling (Fig. 10). The first inch below the contact is exceptionally rich in mordenite.

The core from 125.0 to 171.85 feet is pervasively altered to clinoptilolite, mordenite, celadonite, and montmorillonite. The textural relations are similar to those in the clinoptilolite-bearing core at shallower depths. Mordenite is abundant, primarily as thin fibres in intergranular cavities (Fig. 11).

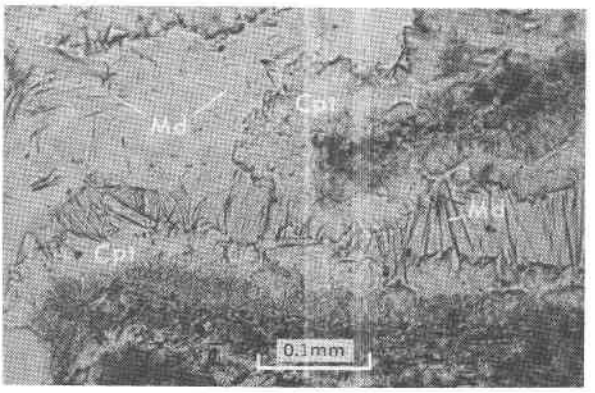

FIG. 11. Photomicrograph of Y1-161 1/2, showing clusters of radiating clinoptilolite crystals (cpt) at edge of an intergranular cavity containing wisps of mordenite (md). At bottom is matrix material composed primarily of clinoptilolite. Plane light.

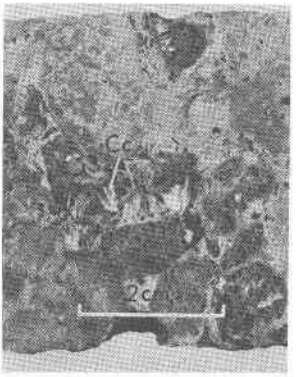

FIG. 12. Photograph of Y1-202.9, showing bladed calcite (cc) in vuggy, leached conglomerate. Cavities contain a network of analcime and quartz crystals.

Analcime does occur at 128.5 feet in the conglomerate near a 2 mm thick fracture filling composed of chalcedony, analcime, celadonite, pyrite, and mordenite. Analcime also occurs at depths greater than 150 feet primarily as fillings of intergranular cavities, but also as euhedral crystals in relict obsidian clasts. Secondary quartz, however, is present only in trace amounts, and α-cristobalite persists in many samples.

The lower contact of this clinoptilolite-bearing zone is again quite abrupt. The contact is at a depositional boundary between light-greenish-gray sandstone above and medium-green siltstone and sandstone below. The hydrothermal minerals immediately above the contact are dominant clinoptilolite, subordinate analcime, and minor mordenite, montmorillonite, and celadonite; α-cristobalite is also present. The hydrothermal minerals immediately below the contact are dominant analcime and quartz, with minor mordenite, montmorillonite, and celadonite. No clinoptilolite was detected in any samples from depths greater than 171.85 feet, and no α-cristobalite from 171.85 to 207 feet (Fig. 2).

The core from 171.85 to 205.0 feet is the most intensely altered core of Y-1. Analcime and hydrothermal quartz are abundant. Celadonite and montmorillonite are present in minor amounts throughout. Clinoptilolite is completely absent, and mordenite is present only to approximately 175 feet. Calcite becomes conspicuous below 177 feet as thin, bladed crystals up to 3 cm across that are intergrown with analcime and quartz in vugs (Fig. 12). At 193–194 feet these calcite crystals have been replaced by chalcedonic quartz.

The core at depths greater than 187 feet is entirely conglomerate and is exceedingly vuggy (Fig. 12). Many of these vugs represent original obsidian clasts that have been leached out by hydrothermal fluids. The original perlitic texture of these relic obsidian grains has been completely

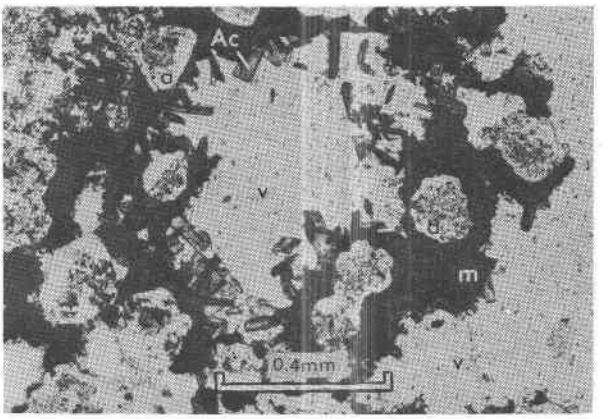

FIG. 13. Photomicrograph of Y1-204.7, showing hydrothermal aegirine (Ac) growing with montmorillonite (m) on hydrothermal analcime (a). Plane light. (v) void space.

obliterated by the hydrothermal alteration. Characteristically, the vugs are lined with euhedral analcime crystals about 0.1–0.25 mm across.

From 204.7 to 205.0 feet, at the bottom of this intensely altered interval, spectacular euhedral crystals of aegirine occur in the analcime-lined cavities. These crystals, up to 0.15 mm long, radiate from individual analcime crystals (Fig. 13) and thus must have been formed subsequent to the analcime and in a hydrothermal environment. To our knowledge this is the first known occurrence of aegirine in a hot-spring system. It should be noted, however, that aegirine has been described as a constituent of scale lining steam boilers down to temperatures below 200°C (Kirsch, 1967, p. 307–309).

The alteration pattern changes abruptly at 205.0 feet. The rock is no longer vuggy but is a dark-green, tough conglomerate that grades downward through a colluvial(?) breccia into bedrock rhyolite. Analcime occurs only in trace quantities below 205 feet, whereas mordenite is present, commonly in veins with chalcedony and subordinate montmorillonite and celadonite (Fig. 14). The mordenite-chalcedony association was nowhere detected at shallower depths. Montmorillonite and celadonite are sporadic. Bladed calcite does not occur below 205.2 feet, but quartz pseudomorphs after bladed calcite were noted at 207.0–207.5 and 208.3–209.3 feet. A single specimen from approximately 207 feet (part of a redrilled interval) displays a vein 7 mm thick consisting of calcite, chalcedony, and mordenite. α-cristobalite was detected sporadically from 205.0 to 211 feet, and is abundant in the rhyolite bedrock from 211 to 215 feet.

The bedrock rhyolite flow from 211 to 215 feet and the fragments derived from this flow that were incorporated into the overlying colluvial(?) breccia and conglomerates display a number of features that are found

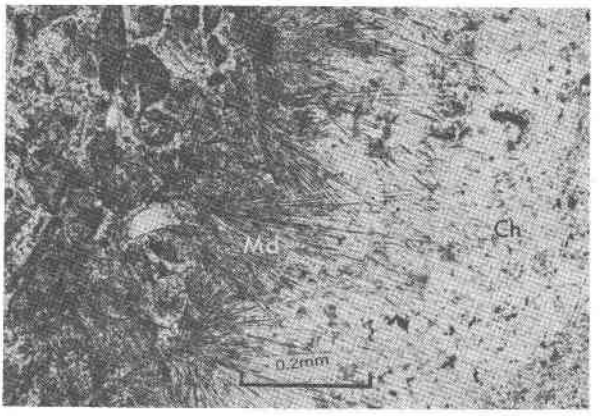

FIG. 14. Photomicrograph of Y1-207, showing mordenite (md) fibers and chalcedony (ch) at edge of fracture filling. Rock at left consists of igneous crystal fragments in a matrix of mordenite, quartz, montmorillonite, and a trace of analcime. Plane light.

nowhere else in Y-1. We interpret many of these features as having been formed during the cooling of this flow and probably not related to the present hydrothermal regime.

This rhyolite flow has phenocryst mineralogy that is unique among Yellowstone flows (R. L. Christiansen, oral commun., 1968). Instead of containing abundant phenocrysts of quartz and sanidine with minor pyroxene and virtually no plagioclase, it contains dominant plagioclase phenocrysts, minor quartz and pyroxene, and little or no sanidine. The phenocrysts are conspicuously glomeroporphyritic, and the plagioclase (andesine) phenocrysts are corroded and embayed. These embayments are commonly filled with groundmass material (alkali feldspar, quartz, and α-cristobalite) or with homogeneous alkali feldspar. Texturally similar alkali feldspar occurs in outcrops away from the hot spring areas and is thus interpreted as a phenomenon of the cooling history of the flow. Alkali feldspar is also present as lath-shaped crystals in cavities; these are interpreted as the product of high-temperature vapor-phase crystallization during cooling of the flow.

Hematite is abundant in this rhyolitic flow rock, mainly as earthy red material disseminated throughout the devitrified groundmass. Hematite also occurs with some green to brown biotitic(?) material along cleavage of plagioclase phenocrysts and in cracks cutting across these phenocrysts.

Chlorite is detected in small quantities on X-ray diffractograms from 205 to 212 feet, and the X-ray data suggest a complementary abundance pattern between chlorite and montmorillonite and/or celadonite. The chlorite was not readily identifiable in thin section, but it probably occurs

primarily as the alteration product of pyroxene phenocrysts, along with 15 Å montmorillonite and biotitic material. The pyroxene phenocrysts do not display the replacement by celadonite that was observed commonly in the sediments.

It is uncertain whether the hematite and the chlorite are products of the present hydrothermal regime or are relicts from earlier deuteric alteration during cooling of the flow.

Hydrothermal quartz, however, is abundant in this flow rock as microcrystalline subhedral crystals lining or filling cavities, into many of which project vapor-phase alkali feldspar crystals. Many of these alkali feldspar crystals are unaltered. Other crystal forms, however, are completely replaced by quartz; the psuedomorphs are outlined by red hematitic material. Some of these pseudomorphs display the habit of tridymite, but the majority are identical in crystal form to the vapor-phase alkali feldspar crystals and appear to be replacements of alkali feldspar by hydrothermal quartz.

Discussion

Detailed discussion of the factors that control hydrothermal mineral assemblages is premature at this time and will be deferred until completion of the work in progress on core from the other 12 drill holes in Yellowstone. However, the distribution of hydrothermal minerals in Y-1 points to the importance of three factors: 1) nature of the starting material, 2) elevated temperature, and 3) fluid composition.

The composition and physical state of the starting material is obviously important in determining whether or not a hydrothermal mineral assemblage can be formed. Obsidian is readily altered, whereas lithoidal rhyolite of essentially identical composition shows few effects other than recrystallization of α-cristobalite to quartz. Likewise, feldspar phenocrysts are resistant to alteration in all but a few samples, and even the pyroxene crystals persist with only partial destruction. Accordingly, the hydrothermal mineral distribution in Y-1 reflects primarily the alteration of obsidian, augmented by deposition of hydrothermal minerals in open spaces. This distribution is not due to variation in original composition of the obsidian with depth, particularly considering the mechanical mixing and homogenization that took place in the erosional and depositional processes.

Elevated temperature was a major factor in the production of alteration minerals in Y-1. Similar sediment and rock in areas of Yellowstone Park affected only by cold water display none of the alteration features of Y-1. Furthermore, throughout the Park both in outcrop and in drill core the amount of alteration correlates rudely with relative nearness to hot-

spring areas. Accordingly, the alteration features of Y-1 could not have been produced by cold ground water prior to establishment of the hot-spring system.

In Y-1, elevated temperatures clearly were of major importance in hastening the crystallization of hydrothermal minerals from obsidian glass, as shown by the nearly complete replacement of obsidian at temperatures above 85°C (Fig. 2). Temperature dependence is also shown by the restriction of opal to temperatures below 104°C, and possibly by the restriction of erionite to temperatures below about 110°C. Other aspects of mineral distribution in Y-1, however, do not correlate with measured ground temperature. Neither the association of clinoptilolite, mordenite, and α-cristobalite nor the association of analcime and quartz is characteristic of a specific temperature interval, and there is no consistent succession of mineral assemblages with increasing depth and temperature.

The chemical composition of the interstitial fluid may well be the most significant variable controlling the mineral assemblages. In many samples the same mineral assemblage occurs replacing obsidian and filling voids. Were this identity due to local uniform temperature, the variations in mineral associations should correlate with temperature, which they do not. Furthermore, the sharp alteration boundaries between the clinoptilolite-bearing rock and the analcime-bearing rock (p. 1722, 1727, and p. 1728) cannot be explained by temperature variation but could be due to abrupt variation in fluid composition. Such variation can be caused by rock-water interaction, variation in rate of fluid flow, varying rates of precipitation from solution, and other kinetic factors. The supersaturated state of the discharging hot-spring waters with respect to α-cristobalite and quartz suggests that the potential for variation of SiO_2 content in response to the above factors is particularly great.

Comparison of opal distribution in Y-1 with data from solubility experiments (Fournier and Rowe, 1966) indicates that silica solubility is indeed an important factor in the interpretation of Y-1. At a silica content of 313 ppm (from Table 1), water should be super-saturated with respect to amorphous silica at temperatures below 93°C (Fournier and Rowe, 1966, Fig. 3). In Y-1, hydrothermal opal is found to a depth of 52.5 feet, corresponding to a temperature of approximately 104°C. This discrepancy may be due to shifting of the saturation curve to higher temperatures owing to the presence of β-cristobalite in the natural opal phase.[1]

The α-cristobalite of Figure 2 is not a hydrothermal product but is

[1] This explanation is supported by unpublished solubility data of R. O. Fournier on a natural mixture of opal and β-cristobalite.

relic from high-temperature crystallization in the flow from which the rhyolite detritus was derived. Inasmuch as quartz is the stable phase at the temperatures and pressures of hydrothermal systems, one might expect α-cristobalite to convert to quartz and the rate of conversion to increase with temperature. Figure 2 shows that α-cristobalite does convert to quartz, but does not suggest a simple temperature dependence. Temperatures of 117°C (or lower) appear to be sufficient to allow recrystallization of α-cristobalite to quartz, but the conversion does not occur uniformly at higher temperatures. At 117°C the saturation point for α-cristobalite is only 165 ppm SiO_2 (Fournier and Rowe, 1966, Fig. 3), about half the SiO_2 content of surface hot-spring water (Table 1). However, hot-spring water expelled at the surface is water that moved rapidly through the hydrothermal system. Perhaps interstitial water in various parts of the system either moves through much more slowly or is involved in local complex circulation or convection patterns. Loss of silica to the rocks by deposition of quartz would decrease the silica content of the fluid to below the α-cristobalite saturation curve. Under this interpretation, such parts of the hydrothermal system would correspond to the quartz-rich zones.

One cannot, however, consider the deposition of SiO_2 solely in terms of the silica species. Perhaps the most striking feature of Figure 2 is the parallel distribution patterns of the silica minerals and the zeolites. In general, α-cristobalite, mordenite, and clinoptilolite occur together but do not occur with the quartz-analcime assemblage. From these patterns we infer that silica concentrations are important in controlling the zeolite assemblages as well as the silica minerals. Clinoptilolite and mordenite seem to occur at higher silica activities, whereas analcime is the zeolite present at silica activities below the α-cristobalite solubility curve. It should be noted that analcime does not occur as a direct alteration of glass, perhaps owing to the role of glass in maintaining a high initial SiO_2 activity and promoting the crystallization of clinoptilolite and mordenite.

It should be emphasized that there is no assurance that the hydrothermal mineral associations of Y-1 are equilibrium assemblages. The natural hot-spring environment may well be similar to the situation encountered in the experimental synthesis of zeolites. Coombs *et al.* (1959, p. 85–86) state that " . . . if attainment of equilibrium is desired the worst possible starting materials are the most reactive, i.e., gels, mixes, and glasses. These are so unstable that a large number of metastable intermediates may form and persist. However, with less unstable starting materials reaction rates are commonly too slow for recrystallization to be achieved." The persistence of unstable phases such as feldspar and

pyroxene in the hydrothermally altered rocks of Y-1 serves to substantiate application of this statement to the natural hydrothermal environment.

The Y-1 alteration pattern displays many similarities to the mineralogical associations formed during the diagenesis of sedimentary rocks rich in silicic volcanic detritus (*cf.* Hay, 1966). Perhaps the most striking resemblance is between the clinoptilolite-bearing rocks of Y-1 and the clinoptilolite facies of the John Day Formation in Oregon (Hay, 1963, p. 217–218). As in the Y-1 rocks, nearly all the glass in the lower 1000–1500 feet of the John Day Formation is replaced by clinoptilolite, montmorillonite, and celadonite. Opal, erionite, and mordenite are also present in both rock suites, but mordenite is present only sporadically in the John Day Formation.

References

Coombs, D. S. (1955) X-ray observations on wairakite and non-cubic analcime. *Mineral. Mag.* **30,** 699–708.

———, A. J. Ellis, W. S. Fyfe, and A. M. Taylor (1959) The zeolite facies, with comments on the interpretation of hydrothermal systems. *Geochim. Cosmochim. Acta,* **17,** 53–107.

———, and J. T. Whetten (1967) Composition of analcime from sedimentary and burial metamorphic rocks. *Geol. Soc. Amer. Bull.* **78,** 268–282.

Evans, H. T., Jr., D. E. Appleman, and D. S. Handwerker (1963) The least squares refinement of crystal unit cells with powder diffraction data by an automatic computer indexing method [abstr.]. *Amer. Crystallogr. Ass., Cambridge, Mass., Ann. Meet., Program,* 42–43.

Fenner, C. N. (1936) Bore-hole investigations in the Yellowstone Park. *J. Geol.,* **44,** 225–315.

Fournier, R. O., and J. J. Rowe (1966) Estimation of underground temperatures from the silica content of water from hot springs and wetsteam wells. *Amer. J. Sci.* **264,** 685–697.

Gude, A. J., and R. A. Sheppard (1967) Composition and genesis of analcime in the Barstow Formation, San Bernardino County, California [abstr.]. *Clays Clay Minerals* **15, (1966),** 189.

Hay, R. L. (1963) Stratigraphy and zeolitic diagenesis of the John Day Formation of Oregon. *Univ. Calif. Pub. Geol. Sci.* **42,** 199–262.

——— (1966) Zeolites and zeolitic reactions in sedimentary rocks. *Geol. Soc. Amer., Spec. Pap.* **85,** 130 p.

Holland, H. D. (1967) Gangue minerals in hydrothermal deposits. *in* H. L. Barnes, (ed.), *Geochemistry of Hydrothermal Ore Deposits.* Holt, Rinehart and Winston, Inc., New York, 382–436.

Kirsch, Helmut (1967) Die Abscheidung fester Phasen aus dem Wasser-Dampf-Kreislauf der Hochdruckdampfkraft-werke und Vergleich dieser Bildungen mit der Minerogenese. *Neues Jahrb. Mineral.* **106,** 287–333.

Nolan, J., and A. D. Edgar (1963) An X-ray investigation of synthetic pyroxenes in the system acmite-diopside-water at 100 kg/cm$_2$ water-vapour pressure. *Mineral. Mag.* **33,** 625–634.

ORVILLE, P. M. (1963) Alkali ion exchange between vapor and feldspar phases. *Amer. J. Sci.* **261,** 201–237.

RICHMOND, G. M. (1965) Glaciation of the Rocky Mountains. *in* H. E. Wright, Jr., and D. G. Frey, (eds.), *The Quaternary of the United States.* Princeton Univ. Press, Princeton, N. J., 217–230.

SAHA, PRASENJIT (1959) Geochemical and X-ray investigation of natural and synthetic analcites. *Amer. Mineral.* **44,** 300–313.

SHEPPARD, R. A., AND A. J. GUDE, 3rd (1969) Diagenesis of tuffs in the Barstow Formation, Mud Hills, San Bernardino, California. *U.S. Geol. Surv. Prof. Pap.* **634,** 35 p.

WISE, W. S., AND H. P. EUGSTER (1964) Celadonite: synthesis, thermal, stability and occurrence. *Amer. Mineral.* **49,** 1031–1083.

WRIGHT, T. L., AND D. B. STEWART (1968) X-ray and optical study of alkali feldspar: I. Determination of composition and structural state from refined unit-cell parameters and 2*V*. *Amer. Mineral.* **53,** 38–87.

YAGI, KENZO (1966) The system acmite-diopside and its bearing on the stability relations of natural pyroxenes of the acmite-hedenbergite-diopside series. *Amer. Mineral.* **51,** 976–1000.

YODER, H. S., AND H. P. EUGSTER (1955) Synthetic and natural muscovite. *Geochim. Cosmochim. Acta,* **8,** 225–280.

APPENDIX—MINERALOGICAL DATA

Clinoptilolite. Clinoptilolite was separated using heavy liquids and magnetic techniques from core from 48 feet, and was analyzed by wet chemical techniques (Table 3). The

TABLE 3. CHEMICAL ANALYSIS OF CLINOPTILOLITE

	(1)	(2)	(3)
SiO_2	63.38%	63.81%	63.74%
TiO_2	n.d.	0	0
Al_2O_3	12.79	13.17	13.15
Fe_2O_3	.46	0	0
MnO	tr.	0	0
MgO	.28	.04	0
CaO	1.31	1.35	1.37
Na_2O	3.50	3.60	3.68
K_2O	3.55	3.37	3.17
H_2O^-	8.79	14.66	14.87
H_2O^+	5.56		
Total	99.84	100.00	99.98

(1) Wet chemical analyses of clinoptilolite containing several percent celadonite. Analysis by Toshio Negishi.

(2) Chemical analyses recalculated to eliminate celadonite, assuming all Fe to be in celadonite of composition $KMgFeSi_4O_{10}(OH)_2$. Calculated celadonite content = 2.5%.

(3) Chemical analysis recalculated to eliminate celadonite, assuming all Fe to be in celadonite of composition $KMgFe_{0.5}Al_{0.5}Si_4O_{10}(OH)_2$. Calculated celadonite content = 4.75%.

TABLE 4. X-RAY DATA FOR ANALCIME

Sample no.	$\Delta 2\theta_{Si_{311}-A_{693}}$	Si per 96 O	R.I. limits
Y1-112	2.10°	35.6	1.4824–1.4846
Y1-117	2.10°	35.6	1.4830–1.4852
Y1-161.4	2.12°	35.8	1.4832–1.4848
Y1-174.4	2.11°	35.7	1.4821–1.4844
Y1-178.0	2.10°	35.6	1.4829–1.4849
Y1-201.5	2.12°	35.8	1.4822–1.4843
Y1-204.7	2.06°	25.2	1.4821–1.4841

analyzed sample contained several percent celadonite, the chemical composition of which is not known precisely. In Table 2 the analysis is recalculated assuming all the iron of the analyzed sample to be in the celadonite and making two extreme assumptions for the composition of the celadonite (from Wise and Eugster, 1964). The β index of refraction of this clinoptilolite is $1.475 \pm .002$.

Several samples from Y-1 contain zoned clinoptilolite (*e.g.*, Fig. 7). In core from 100 feet clinoptilolite replacing sanidine occurs as radial sheaves, the central parts of which have positive elongation with birefringence less than 0.005. The sheaves grade outward with optical continuity through an isotropic zone to clinoptilolite of negative elongation and anomalous brown birefringence. Zoned clinoptilolite has also been found in the Barstow Formation of Southern California (Sheppard and Gude, 1969).

Analcime. Analcime compositions were determined on seven samples using the method of Saha (1959) and the determinative curve of Coombs and Whetten (1967, Fig. 1). At least 4 diffractometer scans at $\frac{1}{4}°$ per minute were made for each sample. The compositions thus determined (Table 4) are almost identical and are as siliceous as any analcime analyses yet reported (cf. Gude and Sheppard, 1967).

X-ray diffraction patterns of several of these analcimes display a weak (200) peak at ~6.8 Å. This reflection is one of those considered by Coombs (1955) to be diagnostic of analcime that is not strictly cubic. We could not detect a 3.21 Å peak, and could detect no splitting of the (332), (422), (431), or (521) reflections.

Montmorillonite. Montmorillonite was concentrated from six samples by hand picking or by elutriation in a beaker. Basal spacing, before and after treatment with ethylene glycol, was measured on oriented smears on glass slides (Table 5). There was no 10 Å mica de-

TABLE 5. X-RAY DATA FOR MONTMORILLONITE

Sample no.	$(001)_{water}$	$(001)_{ethylene\ glycol}$	(060)
Y1-26	12.5 Å	17.3 Å	1.49 Å
Y1-42	11.9	16.8	1.49
Y1-81	11.0–12.0	16.9	1.49
Y1-109	13.6	17.0	1.49
Y1-111	12.6–14.5	16.9	1.49
Y1-113½	12.8	—	1.49

tectable upon glycollation. (060) position, measured on samples in aluminum cell packs, indicates that the montmorillonite is dioctahedral.

Aegirine. Aegirine from Y1-204.7 was identified by both X-ray and optical parameters; 23 peaks from 6.37 Å to 1.53 Å were matched with data given by Nolan and Edgar (1963) for synthetic acmite. The crystals are green, strongly pleochroic, and $\alpha \leqq Z$. If one assumes no components in the pyroxene other than acmite and diopside, the α index of 1.76 plotted on the curve of Yagi (1966) suggests a composition of $Ac_{80}Di_{20}$. Use of Figure 3 of Nolan and Edgar (1963) under the same assumption also suggests a composition greater than 80% acmite.

Manuscript received, February 2, 1970; accepted for publication, April 14, 1970.